

High-Precision Platform Positioning with a Single GPS Receiver

Sunil B. Bisnath and Richard B. Langley

*Geodetic Research Laboratory, Department of Geodesy and Geomatics Engineering,
University of New Brunswick, Fredericton, New Brunswick, Canada.*

BIOGRAPHIES

Sunil Bisnath received an Honours B.Sc. in 1993 and an M.Sc. in 1995 in Surveying Science from the University of Toronto. For the past five years he has been a Ph.D. candidate in the Department of Geodesy and Geomatics Engineering at the University of New Brunswick. During this time he has worked on a variety of GPS-related research and development projects at the Department's Geodetic Research Laboratory, the majority of which have focused on the use of GPS for space applications.

Richard Langley is a professor in the Department of Geodesy and Geomatics Engineering at the University of New Brunswick, where he has been teaching and conducting research since 1981. He has a B.Sc. in applied physics from the University of Waterloo and a Ph.D. in experimental space science from York University, Toronto. Professor Langley has been active in the development of GPS error models since the early 1980s and is a contributing editor and columnist for GPS World magazine.

ABSTRACT

The goal of the research described in this paper is the design of a GPS data processing technique capable of producing high-precision positioning results, regardless of platform dynamics, utilising only a single, high-quality receiver. This is accomplished by combining two processing philosophies: point positioning – making use of precise GPS constellation ephemeris and clock offset information to estimation a single receiver's state; and carrier-phase-filtered, pseudorange processing – supplementing pseudorange-based positioning with carrier-based position-change information.

Results determined via developed software, indicate that near decimetre-level positioning accuracy is attainable for a variety of platforms ranging from static, terrestrial

reference stations, to aircraft, to satellites. A number of modelling improvements can be applied to the existing software, and testing in the real-time environment is planned.

INTRODUCTION

A primary application of GPS is the precise positioning of a myriad of differing user platforms over a broad spectrum of environments, on and above the earth's surface. Current processing techniques rely on relative positioning between receivers, carrier phase ambiguity resolution, differential receiver corrections, or spatial interpolation of receiver network information, implemented in dynamics-tuned filtering schemes to greatly improve position accuracy over that provided by the Standard Positioning Service.

The potential of point positioning is that it can remove these cumbersome aspects of GPS positioning for many applications. The authors have devised a novel approach which obviates the need for these techniques by using data from only the user receiver and products of the International GPS Service (IGS). This approach is not adversely affected by the decorrelation of biases in relative or differential positioning, un-resolved phase ambiguities, spatial interpolation errors, or assumptions regarding platform dynamics, and only requires the tacit assumption of sufficient GPS signals for positioning.

In the following sections point positioning and pseudorange and carrier-phase processing are discussed. Then our single-receiver, platform-independent processing strategy is described. A number of tests with terrestrial, airborne, and spaceborne data are discussed, conclusions are given, and plans for future research are specified.

POINT POSITIONING

The original intent for GPS usage was single-receiver, real-time, pseudorange-based positioning. As is well known, this original design has been altered and enhanced by the use of the carrier-phase observables, relative positioning, and differential positioning on local and wide-area scales. In recent years some researchers have turned their focus to point positioning again. With the proliferation of regional and global networks of geodetic-grade GPS receivers, such as the International GPS Service (IGS) network (see, *e.g.*, Neilan *et al.* [1997]), precise GPS satellite orbits and in some cases precise satellite clock offset estimates derived from such networks have been used to produce precise positioning results with a single-receiver. Mathematically, the GPS satellite ephemeris and clock parameter errors can be removed from the positioning functional model.

Work in this area first centred on pseudorange-based positioning (*e.g.*, Héroux and Kouba [1995] and Gao *et al.* [1997]), and then more recently on pseudorange and carrier-phase processing (*e.g.*, Zumberge *et al.* [1997], Han *et al.* [2001], and Héroux *et al.* [2001]). The carrier-phase strategies have involved the estimation of the receiver state, undifferenced phase ambiguities, and other parameters.

In our approach we have avoided the ambiguity estimation process by utilising adjacent-in-time differenced phase measurements. This represents a form of phase-smoothed pseudorange positioning. The rationale for such a formulation, as will be seen, is to eliminate the necessity for dynamic modelling of the platform.

CARRIER-PHASE FILTERED, PSEUDORANGE PROCESSING

A number of researchers have proposed and/or developed such carrier-phase-filtered, pseudorange processing techniques. Their basic form can be attributed to the seminal work of Hatch [1982]. The crux of carrier and pseudorange combination is the use of averaged noisy code-phase range measurements to estimate the ambiguity term in the precise carrier-phase range measurements. The longer the pseudorange averaging, the better the carrier-phase ambiguity estimate. By performing the filtering in the positioning domain, rather than in the measurement domain, changes to the tracked satellite constellation has little effect as long as a continuous filtered solution is possible. In essence, the pseudoranges provide coarse position estimates and the relative carrier phase measurements provide precise position change estimates. The position change estimates are used to map all of the position estimates to one epoch for averaging.

Similar processing filters with a relative positioning formulation have been described by several authors.

Kleusberg [1986] developed the technique for marine applications utilising the double-differenced pseudorange and carrier-phase observables and the GPS broadcast ephemeris in a sequential, least-squares processor. Yunck *et al.* [1986] proposed this type of filter in the same year for the purpose of geometric GPS-based low earth orbiter (LEO) orbit determination. However, this strategy was abandoned for others, since at the time a global array of terrestrial GPS reference stations did not yet exist to provide sufficiently precise GPS ephemerides and clock estimates. Martín-Neira [Quiles-Blanco and Martín-Neira, 1999] in 1990 developed a Kalman filter-based version of this algorithm.

PHASE-CONNECTED, POINT POSITIONING FILTER DESIGN

We have proposed this form of dynamics-free processing for single-receiver processing, utilizing only readily-available IGS data products and the mobile receiver measurements [Bisnath and Langley, 2001a]. This approach provides for very efficient, straightforward processing and takes full advantage of the precise, three-dimensional and continuous nature of GPS measurements, as well as the existing GPS data infrastructure.

The processing flow of the strategy is shown in Figure 1. The input pseudorange and carrier-phase data are pre-processed to detect outliers, cycle slips, *etc.* and then used to form the processing observables. The mobile receiver position is then estimated with the filter described in the following section. If necessary, an accurate interpolation procedure can be applied to provide the mobile receiver state estimates at non-GPS-measurement epochs.

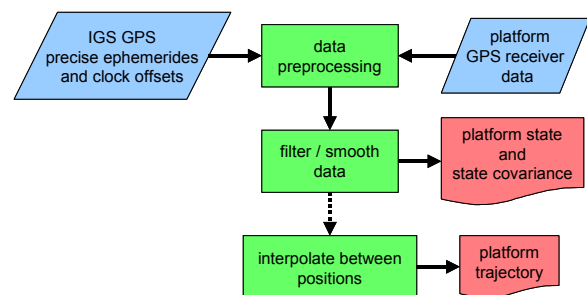


Figure 1: Data processing flowchart of strategy.

The observables fed to the filter are the ionosphere-free, undifferenced pseudorange and the ionosphere-free, time-differenced carrier-phase. For point positioning, a number of additional modelling considerations must be taken into account above and beyond those required for relative positioning (see *e.g.*, Zumberge *et al.* [1997], Witchayangkoon [2000], and Héroux *et al.* [2001]). These include the relativistic GPS satellite clock correction due to the eccentricity in the satellite orbits; GPS satellite antenna phase centre to centre of mass

offset; GPS satellite phase wind-up due to the relative rotation of the satellites with respect to the receiver; sub-diurnal variations in earth rotation; solid earth tides; ocean loading; and consistency between the models used in the generation of the precise GPS orbits and clocks, and those used in the point positioning processing.

FILTER MODELS AND SOLUTION

The linearized filter observation model in matrix form is

$$\begin{bmatrix} \mathbf{P}_t - \mathbf{P}_t^0 \\ \delta\Phi_t - \delta\Phi_t^0 \end{bmatrix} = \begin{bmatrix} 0 & \mathbf{A}_t \\ -\mathbf{A}_{t-1} & \mathbf{A}_t \end{bmatrix} \begin{bmatrix} \delta\mathbf{x}_{t-1} \\ \delta\mathbf{x}_t \end{bmatrix} + \begin{bmatrix} \mathbf{e}_t \\ \boldsymbol{\varepsilon}_{t-1,t} \end{bmatrix};$$

$$\mathbf{C}_{\mathbf{P}_t}, \mathbf{C}_{\delta\Phi_t}, \quad (1)$$

where \mathbf{P}_t and \mathbf{P}_t^0 are the pseudorange measurement and predicted value, respectively; $\delta\Phi_t$ and $\delta\Phi_t^0$ are the time-differenced carrier phase measurement and predicted value, respectively; $\delta\mathbf{x}_{t-1}$ and $\delta\mathbf{x}_t$ are the estimated corrections to the receiver position and clock at epoch $t-1$ and t , respectively; \mathbf{A}_{t-1} and \mathbf{A}_t are the measurement partial derivatives with respect to the receiver position and clock estimates for epochs $t-1$ and t , respectively; \mathbf{e}_t and $\boldsymbol{\varepsilon}_{t-1}$ are the measurement errors associated with \mathbf{P}_t and $\delta\Phi_t$, respectively; and $\mathbf{C}_{\mathbf{P}_t}$ and $\mathbf{C}_{\delta\Phi_t}$ are the covariance matrices for \mathbf{P}_t and $\delta\Phi_t$, respectively. Note that at present the pseudorange and carrier phase measurements are assumed uncorrelated between observables and between observations.

Since the troposphere is a significant contributor to the GPS error budget for platforms within the troposphere, the UNB3 tropospheric prediction model [Collins, 1999] is used. The omission of residual zenith delay estimation causes, on average, approximately few centimetre-level biases in the position estimates. Improved positioning results will be obtained with such estimation.

Another error source not explicitly accounted for in our model is the pseudorange multipath. To mitigate the effect of this phenomenon (see Bisnath and Langley [2001b]) a variant of the pseudorange minus carrier phase linear combination is used to estimate the pseudorange multipath plus noise variance. These variances are used to construct more realistic pseudorange stochastic models.

The *best* solution for (1), in a least-squares sense, is

$$\begin{bmatrix} \hat{\mathbf{x}}_{t-1} \\ \hat{\mathbf{x}}_t \end{bmatrix} = \begin{bmatrix} \mathbf{x}_{t-1}^0 \\ \mathbf{x}_t^0 \end{bmatrix} - \begin{bmatrix} \mathbf{A}_{t-1}^T \mathbf{C}_{\delta\Phi_t}^{-1} \mathbf{A}_{t-1} + \mathbf{C}_{\mathbf{x}_{t-1}}^{-1} & -\mathbf{A}_{t-1}^T \mathbf{C}_{\delta\Phi_t}^{-1} \mathbf{A}_t \\ -\mathbf{A}_t^T \mathbf{C}_{\delta\Phi_t}^{-1} \mathbf{A}_{t-1} & \mathbf{A}_t^T (\mathbf{C}_{\mathbf{P}_t}^{-1} + \mathbf{C}_{\delta\Phi_t}^{-1}) \mathbf{A}_t \end{bmatrix}^{-1} \times \begin{bmatrix} -\mathbf{A}_{t-1}^T \mathbf{C}_{\delta\Phi_t}^{-1} \mathbf{w}_{\delta\Phi} \\ \mathbf{A}_t^T \mathbf{C}_{\mathbf{P}_t}^{-1} \mathbf{w}_{\mathbf{P}} + \mathbf{A}_t^T \mathbf{C}_{\delta\Phi_t}^{-1} \mathbf{w}_{\delta\Phi} \end{bmatrix}, \quad (2)$$

where $\hat{\mathbf{x}} = \mathbf{x}^0 + \delta\mathbf{x}$ (the estimate is equal to the approximate initially assumed value plus the estimated correction); $\mathbf{w}_{\mathbf{P}}$ and $\mathbf{w}_{\delta\Phi}$ are the misclosure vectors for the pseudoranges and time-differenced carrier phases, respectively; and $\mathbf{C}_{\mathbf{x}_{t-1}}$ is the receiver position and clock covariance based on the last epoch's observations.

As can be seen, the position estimate at the previous epoch, $t-1$, is used to estimate the position at epoch t and so on for the moving platform. (2) represents a kinematic, sequential least-squares filter. This filter is a special case of the Kalman filter. Simply put, from (1) the pseudorange measurement contribution

$$\mathbf{P}_t - \mathbf{P}_t^0 = \mathbf{A}_t \delta\mathbf{x}_t + \mathbf{e}_t;$$

$$\mathbf{C}_{\mathbf{P}_t} \quad (3)$$

can be extracted along with the carrier-phase measurement contribution

$$\delta\Phi_t - \delta\Phi_t^0 = -\mathbf{A}_{t-1} \delta\mathbf{x}_{t-1} + \mathbf{A}_t \delta\mathbf{x}_t + \boldsymbol{\varepsilon}_{t-1,t};$$

$$\mathbf{C}_{\delta\Phi_t}. \quad (4)$$

The terms in (3) can be directly mapped to those of the Kalman filter measurement model, and with some rearrangement the terms in (4) can be effectively related to those of the Kalman dynamic model. That is, the kinematic, sequential least-squares tracking filter behaves like a Kalman filter because the carrier phase measurements represent its dynamic model. The filter process is illustrated in Figure 2.

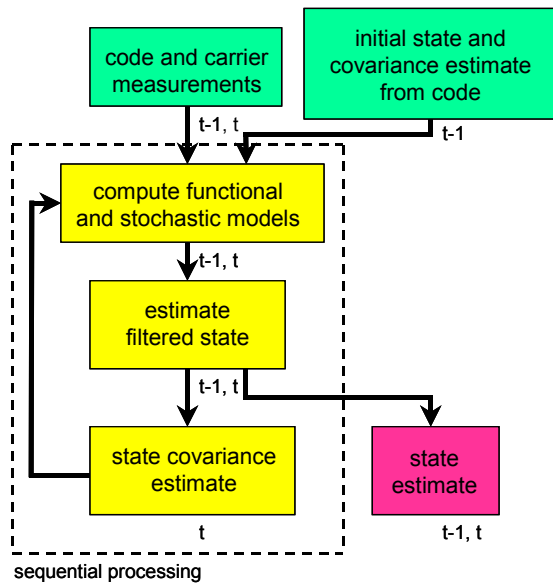


Figure 2: Combination of pseudorange and carrier-phase observations in the kinematic, sequential least squares filter.

Finally, since this tracking strategy is performed after-the-fact and not in real time, data smoothing can be performed. That is, the data arc can be processed in the forward and backward directions and the results can be optimally combined. The smoothed solution is

$$\hat{\mathbf{x}}_s = \mathbf{C}_{f_t}^{-1} \hat{\mathbf{x}}_{f_t} + \mathbf{C}_{b_t}^{-1} \hat{\mathbf{x}}_{b_t}, \quad (5)$$

where $\hat{\mathbf{x}}_s$ is the smoothed parameter estimate, \mathbf{C}_{f_t} is the forward filter parameter covariance, $\hat{\mathbf{x}}_{f_t}$ is the forward filter parameter estimate, \mathbf{C}_{b_t} is the backward filter parameter covariance, and $\hat{\mathbf{x}}_{b_t}$ is the backward filter parameter estimate [Gelb, 1974]. This is a fixed-interval smoother in which the trace of the smoothed parameter covariance matrix is smaller than the trace of the covariance matrices of either filter.

DATA TESTING AND ANALYSIS

In order to validate the viability and performance of this strategy, a number of tests were conducted using the latest version of the developed processing software. This software is based on the University of New Brunswick's scientific GPS processing package DIPOP [Kleusberg *et al.*, 1993] and brought to realisation in the form of a compiled pre-processor and main processor. Even though the code was not designed to be optimal in terms of processing speed, all of the presented results were generated in minutes. Where applicable, mention will be made of additional processing or modelling that, with

future development, will improve the accuracy of the results.

To illustrate the platform-independent nature of the technique, three widely varying types of data have been processed: terrestrial, airborne, and spaceborne. The only common (and required) characteristic of these data sets is that they were collected with geodetic-grade receivers – that is, the receivers were capable of measuring high-quality pseudorange and carrier phase dual-frequency observables. The only other data used in the processing were the requisite IGS precise GPS constellation orbit and high-rate GPS constellation clock offset products.

Static, Terrestrial Data Testing

The objective of the testing with static terrestrial data was to investigate the repeatability of position computations with the technique and to test the performance of the technique against positioning results derived from the highest quality geodetic techniques.

The data used for this testing were collected over a one day period on 5 February 2001 at Natural Resources Canada (NRCan) station Algonquin (IGS station identifier ALGO) in Algonquin Park, Ontario, Canada (latitude 46°N, longitude 78°W). Note that the data set was chosen at random. The NRCan pre-processed TurboRogue BenchMark receiver output contains measurements with a 30 second sampling interval and a 10° elevation mask angle.

As mentioned previously, the currently un-estimated residual tropospheric delay could cause few-centimetre errors in the position domain. The receiver position and clock are estimated at the data sampling interval and this produces a satellite clock modelling error – a few centimetres at the most, arising from interpolating the 300 second interval IGS satellite clocks product. Finally, earth orientation, and carrier phase wind-up have not been accounted for. These components can also produce centimetre-level errors in position, and will be modelled in the near future.

The first aspect of the processing that was analysed, since this technique relies solely on GPS observations, was the geometric strength of the measurements used. Figure 3 shows the number of satellites tracked and the position dilution of precision (PDOP). As can be seen, there are always at least 5 satellites being tracked in this data set and on occasion up to 10. The average number for the processed data is 7.3. The PDOP typically remains between 1.5 and 3, but a few spikes exist where the PDOP reaches approximately 4.5 and 6. The average PDOP is 2.2. Given that there is a 10° elevation mask angle, these values are reasonable and represent geometrically strong measurements. However, given again the complete reliance on measurements, low

elevation angle data, *e.g.*, down to 5°, would have aided in improved accuracy position results.

The results of the processing are presented in Figure 4. The error values are computed by differencing the estimated position from the benchmark International Earth Rotation Service (IERS), epoch-of-date, International Terrestrial Reference Frame 1997 (ITRF97) coordinates. As can be seen, the error in each component reaches a maximum of ± 50 cm. The error fluctuates the most in the vertical component. This is expected, given that the residual tropospheric delay was not estimated, and the inherent limitation brought about by the GPS constellation geometry.

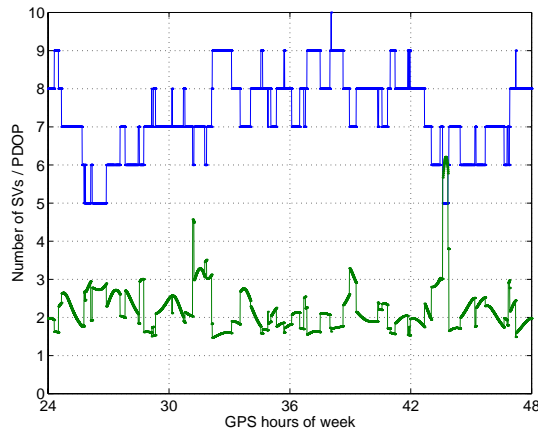


Figure 3: Number of space vehicles (SVs) and the position dilution of precision (PDOP) for static, terrestrial data set.

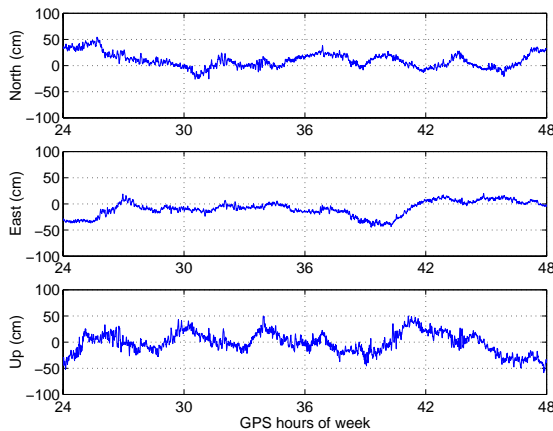


Figure 4: Component errors in smoothed position estimates for static, terrestrial data set.

Summary statistics for this data set are given in Table 1. The r.m.s. of the smoothed solution is 15 cm in each horizontal component, while the vertical component is 20 cm. The smoothed total displacement r.m.s. is just under 30 cm. Also of note are the few-centimetre biases that exist in the horizontal components. Given that the residual tropospheric delay and the sub-daily earth rotation variations have not been applied, and that the GPS satellite orbits and clocks were interpolated to 30 seconds, these results compare favourably with other published single-receiver processing results, *e.g.*, Héroux *et al.* [2001], which show high accuracies. We say this also, since such other published techniques include dynamic information to constrain the solution space – in the case of the mentioned reference, process noise values indicating stationary position.

Component	bias	std.	r.m.s.
North	4.4	13.9	14.5
East	-4.3	14.2	14.8
Up	0.6	19.8	19.8
3-D	6.2	28.0	28.7

Table 1: Summary statistics (cm) of component errors in smoothed position estimates for static, terrestrial data set.

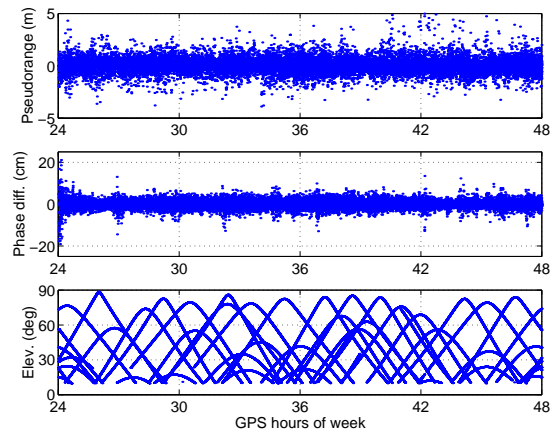


Figure 5: Forward filter observable residuals and associated satellite elevation angles for static, terrestrial data set.

The forward filter residuals, along with the associated GPS satellite elevation angles, are shown in Figure 5. The large initial ionosphere-free, time-differenced phase values are due to filter initialisation. The ionosphere-free pseudorange r.m.s. is 66 cm with peak-to-peak variations of 10 m, and the phase observable r.m.s. is 2 cm with

peak-to-peak variations of 15 cm, aside from the initialisation period. These values appear to be reasonable for the particular linear combinations of the pseudorange and carrier phase combinations they represent.

Airborne Data Testing

The next test illustrates the performance of the processing technique for a receiver on a kinematic platform – a small airplane in level flight in the vicinity of Sendai Airport, in Japan on 5 December 2000. Figure 6 depicts the complete trajectory for the approximately 2 hour flight. The cross pattern of the flight path meant that the aircraft reached a maximum horizontal distance of over 50 km from the cross-over area (Sendai Airport), at which is located a reference receiver that was used for conventional kinematic, relative carrier-phase processing. The conventional solution was obtained with commercial software, using automatic processing parameter settings.

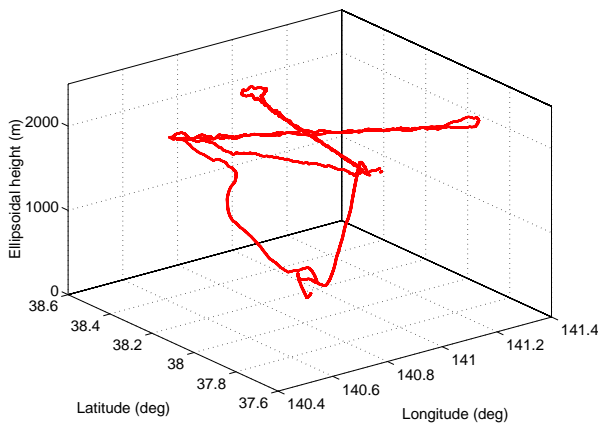


Figure 6: Airborne data set trajectory.

Measurement interruption is a casualty of such level, straight flights with banking turns. As can be seen in Figure 7, the number of tracked satellites is reduced to five or four when the aircraft banks. The actual number can be lower, but data when fewer than four SVs are being tracked are not displayed in Figure 7. The average number of tracked SVs is 6.7. The associated spikes in the PDOP are more acute in this case, since not only are the number of SVs reduced, but their sky distribution is not uniform. Hence, even though the mean PDOP is a respectable 2.4, there are PDOP spikes over 4 during nearly every turn the aircraft makes. This has a significant effect on both the reference double-differenced solution and our single-receiver solution.

Figure 8 shows the differences between the two solutions for one straight-line section of the flight. Table 2 contains the summary statistics of the component differences between the two solutions for this period. The

horizontal components show 50 cm and 70 cm biases in the north and east components, respectively, with standard deviations of 5 cm or less. The up component has a near-one metre drift, causing a 30 cm standard deviation, but very little bias. One possible explanation for the biases and drift can be the use of incorrect double-differenced ambiguities in the commercial software solution. This seems to be a strong possibility for a number of reasons. Firstly, incorrect ambiguities can produce such offsets and drifts. Secondly, offsets and drifts were observed between the used commercial solution and another commercial result. And thirdly, such large biases have not been observed with *any* other data set processed with our technique. These results present another possible use for this technique – the avoidance of incorrectly determined phase ambiguities for long baseline kinematic data sets.

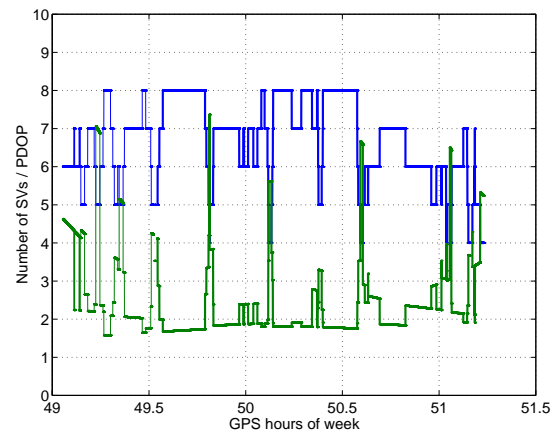


Figure 7: Number of SVs and PDOP for airborne data set.

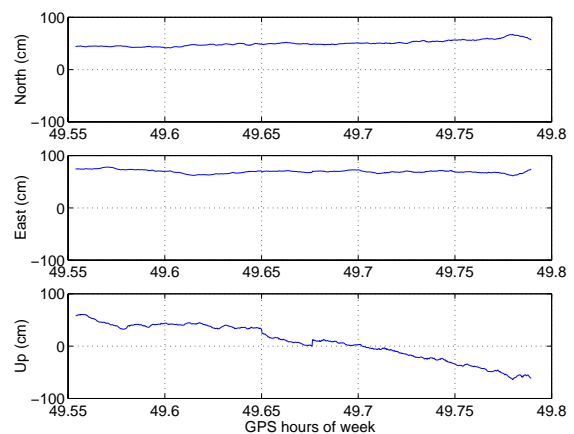


Figure 8: Component differences in smoothed position estimates for airborne data set.

Component	bias	std.	r.m.s.
North	50.3	5.7	50.1
East	69.1	3.0	69.3
Up	7.4	33.4	34.8
3-D	85.8	34.0	92.3

Table 2: Summary statistics (cm) of component differences in smoothed position estimates for airborne data set.

Spaceborne Data Testing

Spaceborne data is unique for a number of reasons. The very high velocity above the atmosphere nature of the platform carrying the receiver means that the tracked GPS satellites change constantly, there is no tropospheric delay on the received signals, high-fidelity dynamic models are typically required for accurate position and orbit determination (especially for LEOs), and given precise orbits, this data type is an excellent benchmark for mobile receiver positioning.

The spaceborne data set processed here consists of three hours of CHAMP [GFZ, 2001] data from 4 June 2001. This LEO orbits at a nominal altitude of 450 km, with a nominal period of 90 minutes, and provides dual-frequency pseudorange and carrier-phase data from a Jet Propulsion Laboratory BlackJack receiver. Figure 9 shows the ground track of the near-polar orbiting spacecraft.

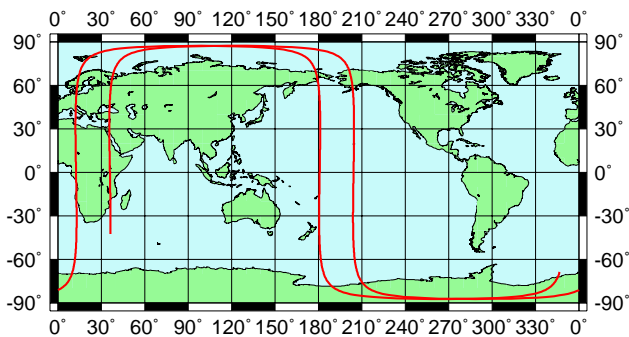


Figure 9: Ground track of CHAMP data set.

The data provided by the CHAMP Data Center is unprocessed and provided at 10 second intervals. No elevation mask angle appears to have been applied, as angles as low as -10° were computed. These very low elevation angle measurements also have very low signal-to-noise (SNR) values (in BlackJack SNR units). It was found that using these measurements produced large phase residuals, and an SNR rather than an elevation

angle cutoff was applied in our data pre-processing to attempt to remedy the situation. The cutoff used in this processing was 10 units.

The purpose of processing these test data was to investigate the geometric strength of the spaceborne measurements and to assess the practicality and performance of the technique against high-quality CHAMP orbits. Figure 10 shows that the geometric strength of the available observations is significantly lower than that for the terrestrial data set we analysed. This occurs, even though the spaceborne BlackJack receiver can track up to 8 GPS satellites and much of the time is tracking the maximum number. The average number of tracked satellites is 6.6. However, the distribution of these tracked satellites causes significant measurement strength degradation. The mean PDOP is 3.1, or almost 50% larger than that for the terrestrial data set processed. This circumstance will be further discussed later in this section.

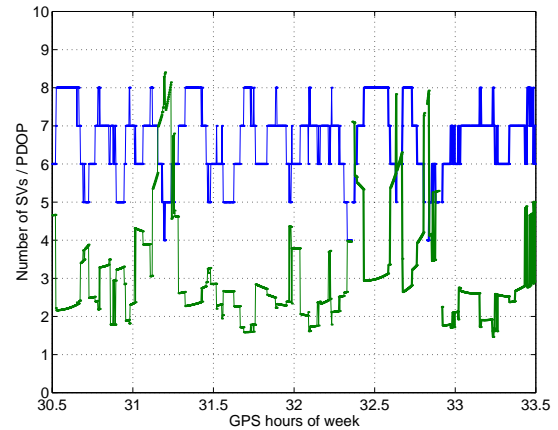


Figure 10: Number of SVs and PDOP for the CHAMP data set.

Figure 11 shows the total displacement difference of our pseudorange-only and smoothed pseudorange/carrier phase solution as compared to the GeoForschungsZentrum-determined dynamic orbit. Only 3-D differences are provided, since the spacecraft attitude information was not used. Note that there are a few small gaps due to the lack of sufficient observations after data pre-processing. Even though the PDOP is relatively high for this data set, the determined pseudorange-only solution is quite accurate as indicated in Table 3. The 3-D r.m.s. is 2 m, which is equivalent to 1.2 m in each axis. The approximate smoothed solution r.m.s. is 20 cm. This difference statistic is judged to be very good, considering that the position accuracy of the dynamic orbit is only somewhat better than 20 cm [Koenig, 2001]. That is, the

phase-connected point positioning results have an r.m.s. similar to that of the benchmark solution.

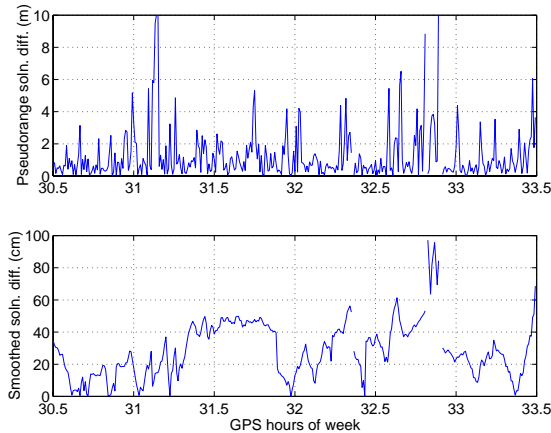


Figure 11: Total displacement errors in position estimates for CHAMP data set.

Sol'n.	Component	bias	std.	r.m.s.
Pseudorange	3-D	125	162	205
	~1-D	72	93	118
Smoothed	3-D	28.7	17.1	33.5
	~1-D	16.5	9.8	19.3

Table 3: Summary statistics (cm) of component differences in pseudorange-only and smoothed position estimates for CHAMP data set.

Figure 12 depicts the forward filter observable residuals and associated GPS satellite elevation angles. Again the data gaps can be clearly seen. The ionosphere-free pseudorange r.m.s. is 90 cm and the ionosphere-free, time-differenced phase r.m.s. is 3 cm. These results compare favourably with those from the terrestrial data set, indicating high-quality observations fitting well with the mathematical and stochastic models.

A property of great interest is the GPS tracking which can be seen in the elevation angle subplot. The very low elevation angle tracking performed by the receiver causes the late tracking of newly rising SVs due to the eight SV hardware limit. Given that a portion of these very low elevation angle measurements are outliers, it would be of great benefit for a GPS-only processing technique, if the low noise, higher elevation angle measurements were collected. This would not only provide more low noise measurements, but more measurements overall, potentially removing most if not all position solution gaps.

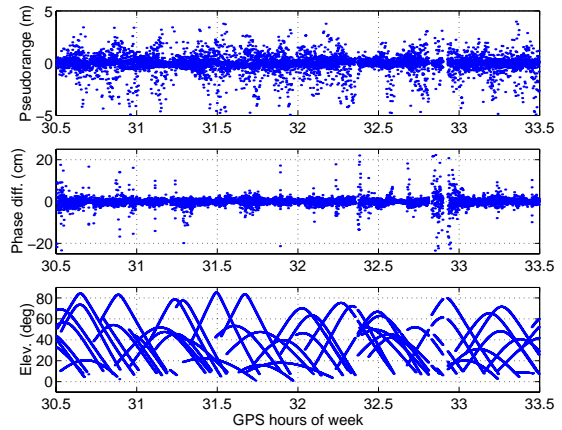


Figure 12: Forward filter observable residuals and associated satellite elevation angles for CHAMP data set.

CONCLUSIONS

A post-processing, platform-independent, single-receiver, positioning strategy based solely on GPS measurements has been devised, which is straightforward, efficient, and fast. The strategy incorporates a kinematic, sequential, least squares filter/smoothers which utilizes the full potential of the GPS measurements, and makes use of readily available GPS data products. As a by-product of the technique's design, its dynamics-free nature allows it to be applied to any platform where sufficient GPS measurements are available.

Static, terrestrial testing results indicate that near decimetre position component r.m.s. and few centimetre position component bias are attainable. These results are seen as promising as there are a number of improvements that have yet to be made in our software. Airborne results are favourable as well, and perhaps emphasize possible risks in long baseline kinematic phase processing. The spaceborne data testing also indicates near-decimetre position component r.m.s. Given all of our test results to date, the goal of decimetre-level position component accuracy is seen as attainable.

FURTHER RESEARCH

A number of additional processing and modelling capabilities are required to refine the present strategy and allow for the most accurate position estimates: modelling of sub-daily earth rotation; phase wind-up; and residual tropospheric delay estimation.

In terms of data processing, more data sets need to be processed to examine the repeatability of these results, and expand the processing capabilities of this technique. Finally, predicted IGS GPS orbits and clocks could be used to attempt real-time precise point positioning.

ACKNOWLEDGEMENTS

Our research was conducted under a grant from the Natural Sciences and Engineering Research Council of Canada. The authors would like to thank the International GPS Service (IGS) for providing the Algonquin Park data set and all of the precise GPS satellite ephemerides and clock offset files; the Electronic Navigation Research Institute, Japan for providing the airborne data set; and the CHAMP Data Center, GeoForschungsZentrum, Germany for providing the spaceborne data set.

REFERENCES

- Bisnath, S.B. and R.B. Langley (2001a). "Precise Orbit Determination of Low Earth Orbiters with GPS Point Positioning." *Proceedings of the Institute of Navigation National Technical Meeting*, The Institute of Navigation, Long Beach, California, U.S.A., 22-24 January, The Institute of Navigation, Alexandria, Virginia, U.S.A., pp. 725-733.
- Bisnath, S.B. and R.B. Langley (2001b). "Pseudorange Multipath Mitigation By Means of Multipath Monitoring and De-Weighting." *Proceedings of the International Symposium on Kinematic Systems in Geodesy, Geomatics and Navigation 2001*, Banff, Alberta, Canada, 5-8 June, 2001, The University of Calgary, Calgary, Alberta, Canada, in press.
- Collins, J.P. (1999). *Assessment and Development of a Tropospheric Delay Model for Aircraft Users of the Global Positioning System*. M.Sc.E. thesis, Department of Geodesy and Geomatics Engineering Technical Report No. 203, University of New Brunswick, Fredericton, New Brunswick, Canada, 174 pp.
- Gao, Y., J.F. McLellan, and M. A. Abousalem (1997). "Single-Point GPS Accuracy Using Precise GPS Data." *The Australian Surveyor*, Vol. 42, No. 4, pp. 185-192.
- Gelb, A. (Ed.) (1974). *Applied Optimal Estimation*. Massachusetts Institute of Technology Press, Cambridge, Massachusetts, U.S.A., 374 pp.
- GFZ (2001). "CHAMP Home Page." http://op.gfz-potsdam.de/champ/index_CHAMP.html. Accessed January 2001.
- Han, S.-C., J. H. Kwon, and C. Jekeli (2001). "Accurate Absolute GPS Positioning Through Satellite Clock Error Estimation." *Journal of Geodesy*, Vol. 75, No. 1, pp. 33-43.
- Hatch, R. (1982), "The Synergism of GPS Code and Carrier Measurements." *Proceedings of the Third International Geodetic Symposium on Satellite Doppler Positioning*, DMA, NOS, Las Cruces, New Mexico, 8-12 February, Physical Science Laboratory, New Mexico State University, Las Cruces, New Mexico, Vol. II, pp.1213-1232.
- Héroux, P. and J. Kouba (1995). "GPS Precise Point Positioning with a Difference." Presented at *Geomatics '95*, Ottawa, Ontario, Canada, 13-15 June.
- Héroux, P., J. Kouba, P. Collins, and F. Lahaye (2001). "GPS Carrier-Phase Point Positioning with Precise Orbit Products." *Proceedings of the International Symposium on Kinematic Systems in Geodesy, Geomatics and Navigation 2001*, Banff, Alberta, Canada, 5-8 June, 2001, The University of Calgary, Calgary, Alberta, Canada, in press.
- Kleusberg, A., Y. Georgiadou, F. van den Heuvel, and P. Héroux (1993). "GPS Data Preprocessing with DIPOP 3.0," internal technical memorandum, Department of Surveying Engineering (now Department of Geodesy and Geomatics Engineering), University of New Brunswick, Fredericton, 84 pp.
- Kleusberg, A. (1986). "Kinematic Relative Positioning Using GPS Code and Carrier Beat Phase Observations," *Marine Geodesy*, Vol. 10, No. 3/4, pp. 257-274.
- Koenig, R. (2001). Personal e-mail, GeoForschungsZentrum, Potsdam, Germany, 9 April.
- Neilan, R.E., J.F. Zumberge, G. Beutler, and J. Kouba (1997). "The International GPS Service: A global resource for GPS applications and research." *Proceedings of the 10th International Technical Meeting of the Satellite Division of the Institute of Navigation*, Kansas City, Missouri, U.S.A., 16-19 September, 1997, The Institute of Navigation, Alexandria, Virginia, U.S.A., Vol. 1, pp. 883-889.
- Quiles-Blanco, A. and M. Martin-Neira (1999). "Performance Comparison Between a Dynamic-Free Navigation Filter and the Carrier Smoothing Algorithm." *Proceedings of the 12th International Technical Meeting of the Satellite Division of The Institute of Navigation*, Nashville, Tennessee, U.S.A., 14-17 September, 1999, The Institute of Navigation, Alexandria, Virginia, U.S.A., pp. 1597-1607.
- Witchayangkoon, B. (2000). *Elements of GPS Precise Point Positioning*. Ph.D. dissertation, Department of Spatial Information Science and Engineering, University of Maine, Orono, Maine, U.S.A., 265 pp.
- Yunck, T. P., S.-C. Wu, and J.-T. Wu (1986). "Strategies for Sub-Decimeter Satellite Tracking with GPS," *Proceedings of IEEE Position, Location, and Navigation Symposium 1986*, Las Vegas, Nevada, U.S.A., 4-7 November, Institute of Electrical and Electronics Engineers, Inc., New York, New York, U.S.A., pp. 122-128.
- Zumberge, J.F., M.B. Heflin, D.C. Jefferson, M.M. Watkins, and F.H. Webb (1997). "Precise Point Positioning for the Efficient and Robust Analysis of GPS Data From Large Networks." *Journal of Geophysical Research*, Vol. 102, No. B3, pp. 5005-5017.